QUASI-OPTIMAL SCHWARZ METHODS FOR THE CONFORMING SPECTRAL ELEMENT DISCRETIZATION

MARIO A. CASARIN*

Abstract. The spectral element method is used to discretize self-adjoint elliptic equations in three dimensional domains. The domain is decomposed into hexahedral elements, and in each of the elements the discretization space is the set of polynomials of degree N in each variable. A conforming Galerkin formulation is used, the corresponding integrals are computed approximately with Gauss-Lobatto-Legendre (GLL) quadrature rules of order N, and a Lagrange interpolation basis associated with the GLL nodes is used. Fast methods are developed for solving the resulting linear system by the preconditioned conjugate gradient method. The conforming *finite element* space on the GLL mesh, consisting of piecewise Q_1 or P_1 functions, produces a stiffness matrix K_h that is known to be spectrally equivalent to the spectral element stiffness matrix K_N. K_h is replaced by a preconditioner $\tilde{K}_h$ which is well adapted to parallel computer architectures. The preconditioned operator is then $\tilde{K}_h^{-1}K_N$.

Our techniques for non-regular meshes make it possible to estimate the condition number of $\tilde{K}_h^{-1}K_N$, where $\tilde{K}_h$ is a standard finite element preconditioner of K_h, based on the GLL mesh. The analysis of two finite element based preconditioners: the wirebasket method of Smith, and the overlapping Schwarz algorithm for the spectral element method, are given as examples of the use of these tools. Numerical experiments performed by Pahl are briefly discussed to illustrate the efficiency of these methods in two dimensions.

Key words. domain decomposition, Schwarz methods, spectral element method, preconditioned conjugate gradients, iterative substructuring

AMS(MOS) subject classifications. 41A10, 65N30, 65N35, 65N55

1. Introduction. The spectral element method has been used extensively to discretize a variety of partial differential equations, and its efficiency has been demonstrated both analytically and numerically; see [18, 19], and references therein. It uses polynomials of high degree in each element, and a particular choice of basis and numerical quadrature rules. In large scale problems, long range interactions between the basis elements within each substructure produce quite dense and expensive factorizations of the stiffness matrix, and the use of direct methods is often not economical because of the large memory requirements [14]. In the past decade, many preconditioners have been developed for *finite element* discretizations of these equations; see e.g. [16, 17, 29]. For both families of discretizations, the design of preconditioners for three dimensional problems is especially challenging.

Early work on preconditioners for spectral methods was carried out by Canuto and Funaro [7] and Pavarino [24, 25, 26]. Some of the algorithms studied by Pavarino are numerically scalable (i.e., the number of iterations is independent of the number of substructures) and optimal (the number of iterations does not grow or grows only slowly with the degree of the polynomials). However, each application of his preconditioners can be very expensive.

Several iterative substructuring methods, which preserve quasi-optimality and scalability, were later introduced by Pavarino and Widlund [27, 28]. These preconditioners can be viewed as block-Jacobi methods after the stiffness matrix has been transformed

* Courant Institute of Mathematical Sciences, New York University, 251 Mercer Street, New York, N.Y. 10012. Electronic mail address: casarin@cims.nyu.edu. This work has been supported in part by a Brazilian graduate student fellowship from CNPq, in part by the National Science Foundation under Grant NSF-CCR-9204255, and in part, by the U. S. Department of Energy under contracts DE-FG02-92ER25127.

by using a certain basis. The subspaces used are the analogues of those proposed by Smith [31] for piecewise linear finite element discretizations. The bound for the condition number of the preconditioned operator grows only slowly with the polynomial degree, and is independent of the number of substructures.

The tensorial character of the spectral element matrix can be exploited when evaluating its action on a vector [19], but does not help when evaluating the action of the inverse of blocks of this matrix, as required when using these preconditioners. Orzag [21] and Deville and Mund [8] proposed the use of a finite difference and a Q_1 or P_1 finite element model, respectively, as preconditioners for the spectral element matrix. The triangulation for this finite element method is based on the hexahedrals of the Gauss-Lobatto-Legendre (GLL) mesh of one element. This preconditioner has been demonstrated both numerically, in [8], and theoretically, by Canuto [6], to have a condition number independent of the degree of the polynomials. We note that ideas similar to those in [6] and [8] also appear in Quarteroni and Zampieri [30] and references therein. The spectral equivalence results of Canuto [6] and generalizations for other boundary conditions were also obtained independently by Parter and Rothman [23].

Based on these ideas, extended to the case of several elements, Pahl [22] proposed efficient, easily parallelizable preconditioners for the spectral element method using iterative substructuring or overlapping Schwarz methods applied to the GLL finite element model. Pahl also performed experiments for a model problem in two dimensions, demonstrating that this kind of preconditioner can be very efficient. In other words, high order accuracy is combined with efficient and inexpensive low-order preconditioning. The work of Pahl, however, did not contain any rigorous theoretical justification for the experimental results he obtained.

The previous analysis of Schwarz preconditioners for the h-method has relied upon the shape-regularity of the mesh, see [3, 10, 12], which does not hold at all for the GLL mesh. In this paper, we analyze some Schwarz finite element preconditioners defined on this mesh, and derive polylogarithmic bounds on the condition number of the preconditioned operators for iterative substructuring methods, and a result analogous to the standard finite element bound for overlapping Schwarz algorithms. Then, by applying Canuto's result, [6], we propose and analyze a new overlapping preconditioner that uses only blocks of the spectral element matrix to define the local contributions of the preconditioner. We also give a new proof of one of the estimates in [27]. In summary, the equivalence between the spectral and finite element matrices, and the tools we develop here, allow us to extend the analysis available for the domain decomposition preconditioners of the standard finite element case to the spectral element case. We remark that our techniques may also be used to estimate the convergence of a large class of domain decomposition preconditioners on some non-regular meshes.

The remainder of the paper is organized as follows. The next section contains some notation and a precise description of the discrete problem. The motivation and strategy of this paper are presented in detail in Section 3. In Section 4, we state and prove our technical results. In sections 5 and 6, we formulate and analyze several representative iterative substructuring and overlapping algorithms. Section 7 briefly describes some numerical experiments performed by Pahl [22].

2. Differential and Discrete Model Problems. Let Ω be a bounded polyhedral region in $\mathbb{R}^3$ with diameter of order 1. We consider the following elliptic self-adjoint problem:

Find $u \in H_0^1(\Omega)$ such that

$$a(u,v) = f(v) \quad \forall\, v \in H_0^1(\Omega), \tag{1}$$

where

$$a(u,v) = \int_\Omega k(x)\, \nabla u \cdot \nabla v \, dx \quad \text{and} \quad f(v) = \int_\Omega f v \, dx \quad \text{for } f \in L^2(\Omega).$$

Our results are also valid for mixed Neumann–Dirichlet boundary conditions, but we restrict ourselves to homogeneous Dirichlet conditions. The extension to other self-adjoint cases is routine, and would only add distracting complications to our description. This problem is discretized by the spectral element method (SEM); see [19]. In what follows, the elements of the SEM are denoted by *substructures* or *subdomains*. Later on, we will further divide the substructures into hexahedrals, which will then be called *elements*. They form the triangulation for a finite element space which will be defined momentarily.

We triangulate Ω into non-overlapping substructures $\{\Omega_i\}_{i=1}^M$ of diameter on the order of H. Each Ω_i is the image of the reference substructure $\hat{\Omega} = [-1,+1]^3$ under a mapping $F_i = D_i \circ G_i$ where D_i is an isotropic dilation and G_i a C^∞ mapping such that its Jacobian and inverse of its Jacobian are uniformly bounded by a constant. In Section 3, we show that the bounds that we derive depend on this constant, and are better the closer this constant is to one, i.e. the closer the substructures are to a cube. Moreover, we suppose that the intersection between the closures of two distinct substructures is either empty, a vertex, a whole edge or a whole face. Some additional properties of the mappings F_i are required to guarantee an optimal convergence rate. We refer to [1], problem 2, and references therein for further further details on this issue, but remark that affine mappings are covered by the available convergence theory for these methods. We assume for simplicity that $k(x)$ has the constant value $k_i > 0$ in the substructure Ω_i, with possibly large jumps occurring only across substructure boundaries. The bounds for the iterative substructuring methods are independent of these jumps. For the overlapping methods, we need to introduce more stringent restrictions on $k(x)$ to obtain bounds that are independent of the jumps; see the discussion after Lemma 4.

We define the space $P^N(\hat{\Omega})$ as the space of polynomials of degree at most N in each of the variables separately. The space $P^N(\Omega_i)$ is the space of functions v_N such that $v_N \circ F_i$ belongs to $P^N(\hat{\Omega})$. The conforming discretization space $P_0^N(\Omega) \subset H_0^1(\Omega)$ is the space of continuous functions the restrictions of which to Ω_i belong to $P^N(\Omega_i)$.

The discrete L^2 inner product is defined by

$$(u,v)_N = \sum_{i=1}^{K} \sum_{j,k,l=0}^{N} k_i \cdot (u \circ F_i) \cdot (v \circ F_i) \cdot |J_i|(\xi_j, \xi_k, \xi_l) \cdot \rho_j \rho_k \rho_l, \tag{2}$$

where ξ_j and ρ_j are, respectively, the Gauss-Lobatto-Legendre quadrature points and weights of degree N in the interval $[-1,+1]$; see [1]. We define a discrete bilinear form for $u, v \in H^1(\Omega)$ by

$$a_Q(u,v) = (\nabla u, \nabla v)_N, \tag{3}$$

where $(\cdot,\cdot)_N$ is computed componentwise.

The discrete problem is:
Find $u_N \in P_0^N(\Omega)$, such that

$$a_Q(u_N, v_N) = (f, v_N)_N \quad \forall\ v_N \in\ P_0^N(\Omega). \tag{4}$$

We number the GLL nodes of all the substructures, and choose as basis functions the functions ϕ_j^N of $P_0^N(\Omega)$ that are one at the GLL node j and zero at all the others. This basis gives rise, in the standard way, to the linear system $K_N x = b$. Note that the mass matrix of this nodal basis, generated by the discrete L^2 inner product (2), is diagonal. The analysis and experimental evidence show that the SEM method just described achieves very good accuracy for reasonably small N for a wide range of problems; see [1, 18, 19] and references therein. The practical application of this method for large scale problems, however, depends on fast and reliable solution methods for the system $K_N x = b$. A direct method is often not an economical choice, because of long range interactions between the basis elements, and because this is a discretization of a three dimensional problem, which demands large computer resources even for the seven-point finite difference stencil; see [13].

The condition number of K_N is very large even for moderate values of N; see [1]. Our approach is to solve this system by a preconditioned conjugate gradient algorithm. The following low-order discretization is used to define several preconditioners in the next sections.

The GLL points of degree N, denoted GLL(N), define, in a natural way, a triangulation $\mathcal{T}^{\hat{h}}$ of $\hat{\Omega}$ into N^3 parallelepipeds, and on this triangulation we define the space $P^{\hat{h}}(\hat{\Omega})$ of continuous functions that are trilinear (Q_1) in each parallelepiped of $\mathcal{T}^{\hat{h}}$. The spaces $P^h(\Omega_i)$ and $P_0^h(\Omega)$ are defined by mapping in the same way as for $P^N(\Omega_i)$ and $P_0^N(\Omega)$. The finite element discrete problem associated with (1) is:
Find $u_h \in P_0^h(\Omega)$, such that

$$a(u_h, v_h) = f(v_h) \quad \forall\ v_h \in\ P_0^h(\Omega). \tag{5}$$

The standard nodal basis $\{\hat{\phi}_j^{\hat{h}}\}$ of $P^{\hat{h}}(\hat{\Omega})$ is mapped by the F_i into a basis for $P^h(\Omega_i)$, for $1 \le i \le M$. These bases and the bilinear form $a(\cdot,\cdot)$ give rise to a system $K_h x = b$.

We could also define a finite element system generated by dividing each hexahedral of $\mathcal{T}^{\hat{h}}$ into tetrahedrals, and using P_1 finite elements on this new triangulation. The analysis for P_1 elements carries over immediately from the analysis for Q_1 elements, since the L^2- and H_1-norms are equivalent element by element. We remark that the P_1 elements have been shown to produce smaller condition numbers when used as a preconditioner, and should be prefered in a practical implementation. For the sake of simplicity, we restrict ourselves to the case of Q_1 elements.

We use the following notations: $x \preceq y$, $z \succeq u$, and $v \asymp w$ to express that there are strictly positive constants C and c such that

$$x \le C\,y, \qquad z \ge c\,u, \qquad \text{and} \qquad c\,w \le v \le C\,w, \quad \text{respectively.}$$

Here and elsewhere c and C are moderate constants independent of H, N, and $k(x)$.

Let $\hat{h}$ be the distance between the two leftmost GLL(N) points ξ_0 and ξ_1 in the interval $[-1, +1]$; $\hat{h}$ is on the order of $1/N^2$, while the distance between two consecutive GLL points increases to a maximum, close to the origin, which is on the order of $1/N$;

see [1]. Hence, the aspect ratios of some of the elements of the triangulation $\mathcal{T}^{\hat{h}}$ grow in proportion to N.

For a region of diameter H, such as a substructure Ω_j, we use a norm with weights generated by dilation starting from a region of unit diameter,

$$\|u\|^2_{H^1(\Omega_j)} = |u|^2_{H^1(\Omega_j)} + \frac{1}{H^2}\|u\|^2_{L_2(\Omega_j)},$$

where $|\cdot|_{H^1}$ stands for the H^1-semi-norm.

3. General Strategy and Simplifications. Let $\hat{u}_N$ belong to $P^N(\hat{\Omega})$, and let $\hat{u}_h = \hat{I}^h_N(\hat{u}_N)$ be the unique function of $P^{\hat{h}}(\hat{\Omega})$ for which

$$\hat{u}_h(x_G) = \hat{u}_N(x_G),$$

for every GLL(N) point $x_G \in \overline{\hat{\Omega}}$. Then, by corollary 1.13, page 75 of [1] and the results in [6], we have:

$$||\hat{u}_h||^2_{L^2(\hat{\Omega})} \asymp ||\hat{u}_N||^2_{L^2(\hat{\Omega})} \asymp (\hat{u}_N, \hat{u}_N)_N, \tag{6}$$

and

$$|\hat{u}_h|^2_{H^1(\hat{\Omega})} \asymp |\hat{u}_N|^2_{H^1(\hat{\Omega})} \asymp a_{\hat{Q}}(\hat{u}_N, \hat{u}_N), \tag{7}$$

where $a_{\hat{Q}}$ is given by (2) and (3) with $J_i \equiv 1$ and $k_i = 1$. The basis of the proof of this last result is the H^1-stability of the polynomial interpolation operator at the GLL nodes for functions in $H^1([-1,+1])$, proved by Bernardi and Maday [2, 1]. The L^2-stability of the GLL quadrature of order N for polynomials of degree N, and properties of the GLL nodes and weights are also important in the argument. We remark that the first equivalence of (7) and generalizations to other boundary conditions were obtained independently by Parter and Rothman [23].

Consider now a finite element function u defined in a substructure Ω_i with diameter of order H. Changing variables to the reference substructure by $\hat{v}(\hat{x}) = v(F_i(\hat{x}))$, and using the bounds on the Jacobian of F_i, we obtain

$$\|u\|^2_{L^2(\Omega_i)} \asymp H^d\|\hat{u}\|^2_{L^2(\hat{\Omega})}, \tag{8}$$

and

$$|u|^2_{H^1(\Omega_i)} \asymp H^{d-2}|\hat{u}|^2_{H^1(\hat{\Omega})}, \tag{9}$$

where d is the dimension and is equal to 1, 2, or 3.

These estimates can be viewed as spectral equivalences of the stiffness and mass matrices generated by the norms and the basis introduced above. Indeed, the nodal basis $\{\hat{\phi}^{\hat{h}}_j\}$ is mapped, by interpolation at the GLL nodes, to the nodal basis of $P^N(\hat{\Omega})$. Then, (7) can be written as

$$\underline{\hat{u}}^T \hat{K}_h \underline{\hat{u}} \asymp \underline{\hat{u}}^T \hat{K}_N \underline{\hat{u}}, \tag{10}$$

where $\underline{\hat{u}}$ is the vector of nodal values of both $\hat{u}_N$ or $\hat{u}_h$, and $\hat{K}_h$ and $\hat{K}_N$ are the stiffness matrices associated with $|\cdot|^2_{H^1(\hat{\Omega})}$ and $a_{\hat{Q}}(.,.)$.

Let $K_h^{(i)}$ and $K_N^{(i)}$ be the stiffness matrices generated by the bases $\{\phi_j^h\}$ and $\{\phi_j^N\}$, respectively, for all nodes j in the closure of Ω_i, and by using $|\cdot|^2_{H^1(\Omega_i)}$ and $a_{Q,\Omega_i}(\cdot,\cdot)$, respectively. Here, $a_{Q,\Omega_i}(\cdot,\cdot)$ is the restriction of $a_Q(\cdot,\cdot)$ to the subdomain Ω_i. If $\underline{u}$ is the vector of nodal values, and $\underline{u}^{(i)}$ is its restriction to $\overline{\Omega}_i$, then

$$\underline{u}^{(i)^T} K_h^{(i)} \underline{u}^{(i)} \asymp \underline{u}^{(i)^T} K_N^{(i)} \underline{u}^{(i)},$$

by (7) and (9). The stiffness matrices K_N and K_h are formed by subassembly [10]:

$$\underline{u}^T K_h \underline{u} = \Sigma_i \quad \underline{u}^{(i)T} K_h^{(i)} \underline{u}^{(i)}; \tag{11}$$

an analogous expression holds for K_N. These last two relations imply that

$$\underline{u}^T K_h \underline{u} \asymp \underline{u}^T K_N \underline{u}. \tag{12}$$

This shows that K_h is an optimal preconditioner for K_N in terms of number of iterations. All these matrix equivalences, and their analogues in terms of norms, are hereafter called the FEM-SEM equivalence.

We next show that the same results also hold for the Schur complements S_h and S_N. The *interface* of the decomposition is defined as $\Gamma = \cup_{i=1}^M \partial\Omega_i \setminus \partial\Omega$. The Schur complement matrices S_h and S_N are obtained by the elimination of the interior nodes of each Ω_i by Cholesky's algorithm; see [10]. A function u_N is said to be (piecewise) Q-discrete harmonic if $a_{Q,\Omega_i}(u_N, v_N) = 0$, for all i and all v_N belonging to $P^N(\Omega_i) \cap H_0^1(\Omega_i)$. The definition of (piecewise) h-discrete harmonic functions is analogous. It is clear that $\underline{u}_\Gamma^T S_N \underline{u}_\Gamma = a_Q(u_N, u_N)$ and that $\underline{u}_\Gamma^T S_h \underline{u}_\Gamma = a(u_h, u_h)$, where u_h and u_N are respectively $h-$ and $Q-$discrete harmonic and $\underline{u}_\Gamma$ is the vector of nodal values on Γ of u_h and u_N.

The matrices S_h and S_N are spectrally equivalent. Indeed, by subassembly (11), it is enough to verify the spectral equivalence for each substructure separately. For the substructure Ω_i, we find:

$$\begin{aligned} \underline{u}_\Gamma^{(i)^T} S_N^{(i)} \underline{u}_\Gamma^{(i)} = a_{Q,\Omega_i}(u_N, u_N) \succeq a_{\Omega_i}(I_N^h(u_N), I_N^h(u_N)) \geq \\ a_{\Omega_i}(\mathcal{H}_h(I_N^h u_N), \mathcal{H}_h(I_N^h u_N)) = a_{\Omega_i}(u_h, u_h) = \underline{u}_\Gamma^{(i)^T} S_h^i \underline{u}_\Gamma^{(i)}, \end{aligned} \tag{13}$$

where $\mathcal{H}_h$ is the h-discrete harmonic extension of the interface values, and I_N^h is the composition of $\hat{I}_N^h$ with F_i. Here, we have used the FEM-SEM equivalence and the well-known minimizing property of the discrete harmonic extension. The reverse inequality is obtained in the same way.

This equivalence implies that S_h is an optimal preconditioner for S_N, in terms of number of iterations. However, as before, the action of the inverse of S_h is too expensive to produce an efficient preconditioner for large problems.

In his Master's thesis [22], Pahl proposed the replacement of K_h and S_h by preconditioners $\tilde{K}_h$ and $\tilde{S}_h$, respectively. If the condition number satisfies

$$\kappa(\tilde{K}_h^{-1} K_h) \leq C(N), \tag{14}$$

with a moderately increasing function $C(N)$, then a simple Rayleigh quotient argument shows that $\kappa(\tilde{K}_h^{-1} K_N) \preceq C(N)$; an analogous bound can be derived for $\tilde{S}_h^{-1}$ and S_N. $\tilde{K}_h$ and $\tilde{S}_h$ are domain decomposition preconditioners based on $\mathcal{T}^h$, and are designed so that the action of their inverse on a vector is inexpensive to evaluate.

In the next three sections, we define our preconditioners and then establish (14) and its analogue for S_h and $\tilde{S}_h^{-1}$. We note that the triangulation $\mathcal{T}_h$ is not shape-regular, and that all the bounds of this form for Schwarz preconditioners established in the literature require some kind of inverse condition, or regularity of the triangulation, which, as pointed out in Section 2, does not hold for the GLL mesh.

4. Technical Results. In this section, we present the technical lemmas needed to prove our results. As is clear from the start, we draw heavily upon the results and techniques of Dryja, Smith, and Widlund [10].

4.1. Some estimates for non-regular triangulations. In this section, we develop all the estimates necessary to extend the technical tools developed in [10] to the case of non-regular hexahedral triangulations. We recall that $\hat{\Omega} = [-1,+1]^3$ is the reference *substructure*, and $\mathcal{T}^{\hat{h}}$ its triangulation generated by the GLL mesh. Let $\breve{K} = [-1,+1]^3$ be the reference *element*, and let $\hat{K} \subset \hat{\Omega}$ be a parallelepiped of $\mathcal{T}^{\hat{h}}$ with sides h_1, h_2 and h_3; these mesh parameters are not necessarily comparable in size. The function $\hat{u}$ is a trilinear (Q_1) function defined in $\hat{K}$. In this subsection, we use hats to represent functions defined in $\hat{K}$, and no superscript for points of $\hat{K}$.

Our first result concerns expressions of the $L^2(\hat{K})$- and $H^1(\hat{K})$-norms of a trilinear function $\hat{u}$ in terms of its nodal values. Let e_i be one of the coordinate directions of $\hat{K}$, and let a, b, c and d be the vertices of one of the faces that are perpendicular to e_i. Let a', b', c', and d' be the corresponding points on the parallel face. x_α denotes a generic vertex of $\hat{K}$.

LEMMA 1. *Let $\hat{u}$ be trilinear in $\hat{K}$. Then,*

$$\|\hat{u}\|^2_{L^2(\hat{K})} \asymp h_1 h_2 h_3 \sum_{x_\alpha \in \hat{K}} (\hat{u}(x_\alpha))^2, \tag{15}$$

and

$$\|\partial_{x_i} \hat{u}\|^2_{L^2(\hat{K})} \asymp \frac{h_1 h_2 h_3}{h_i^2} \sum_{x_\alpha = a,b,c,d} (\hat{u}(x_\alpha) - \hat{u}(x'_\alpha))^2. \tag{16}$$

Proof. These formulas follow by changing variables, and by using the equivalence of any pair of norms in the finite dimensional space $Q_1(\breve{K})$. □

In the next lemma, we give a bound on the gradient of a trilinear function in terms of bounds on the differences of the nodal values. Its proof is routine.

LEMMA 2. *Let $\hat{u}$ be trilinear in $\hat{K}$ such that $|\hat{u}(a) - \hat{u}(b)| \leq C|a-b|/r$ for some constant C and parameter r, and for any two vertices a and b belonging to one face of $\hat{K}$. Then*

$$|\nabla \hat{u}| \leq \frac{C}{r},$$

where C is independent of the parameter r.

LEMMA 3. *Let $\hat{u}$ be a trilinear function defined in $\hat{K}$, and let $\hat{\vartheta}$ be a C^1 function such that $|\nabla \hat{\vartheta}| \leq C/r$, and $|\hat{\vartheta}| \leq C$ for some constant C and parameter r. Then*

$$|\partial_{x_i} I^{\hat{h}}(\hat{\vartheta}\hat{u})|^2_{L^2(\hat{K})} \leq C(|\hat{u}|^2_{H^1(\hat{K})} + r^{-2}\|\hat{u}\|^2_{L^2(\hat{K})}). \tag{17}$$

Here C is independent of N and r, and $I^{\hat{h}}$ is the Q_1-interpolant using the values at the vertices of $\hat{K}$.

Proof. By equation (16), and letting h_1, h_2, and h_3 be the sides of the element $\hat{K}$:

$$||\partial_{x_i} I^{\hat{h}}(\hat{\vartheta}\hat{u})||^2_{L^2(\hat{K})} \preceq \frac{h_1 h_2 h_3}{h_i^2} \sum_{x=a,b,c,d} (\hat{u}(x)\hat{\vartheta}(x) - \hat{u}(x')\hat{\vartheta}(x'))^2$$

Each term in the sum above can be bounded by

$$\begin{aligned}\left(\hat{u}(x)\hat{\vartheta}(x) - \hat{u}(x)\hat{\vartheta}(x') + \hat{u}(x)\hat{\vartheta}(x') - \hat{u}(x')\hat{\vartheta}(x')\right)^2 \leq \\ 2\left((\hat{u}(x))^2(\hat{\vartheta}(x) - \hat{\vartheta}(x'))^2 + (\hat{u}(x) - \hat{u}(x'))^2(\hat{\vartheta}(x'))^2\right)\end{aligned}$$

The bound on $\nabla\hat{\vartheta}$ implies that $|\hat{\vartheta}(x) - \hat{\vartheta}(x')| \preceq h_i/r$, and therefore

$$\begin{aligned}||\partial_{x_i} I^{\hat{h}}(\hat{\vartheta}\hat{u})||^2_{L^2(\hat{K})} &\preceq \frac{h_1 h_2 h_3}{h_i^2}\Big(\sum_{x=a,b,c,d} (\hat{u}(x) - \hat{u}(x'))^2 + \sum_{x=a,b,c,d} (\hat{u}(x))^2 \frac{h_i^2}{r^2}\Big) \\ &\preceq |\hat{u}|^2_{H^1(\hat{K})} + r^{-2}||\hat{u}||^2_{L^2(\hat{K})}, \qquad (18)\end{aligned}$$

since $\hat{\vartheta}$ is bounded. □

4.2. Further technical tools. The iterative substructuring algorithms are based on subspaces directly related to the interiors of the substructures, and the faces, edges and vertices. Let Ω_{ij} be the union of two substructures Ω_i, Ω_j, and their common face $\mathcal{F}_k$. Let $\mathcal{W}_j$ represent the wirebasket of the subdomain Ω_j, i.e. the union of all its edges and vertices. We note that a face in the interior of the region Ω is common to exactly two substructures, an interior edge is shared by more than two, and an interior vertex is common to still more substructures. All the substructures, faces, and edges are regarded as open sets.

The following observations greatly simplify our analysis in the next sections. The preconditioner $\tilde{S}_h$ that we propose is defined by subassembly of the matrices $\tilde{S}_h^{(i)}$; see Section 5. We then restrict our analysis to one substructure. The results for the whole region follow by a standard Rayleigh quotient argument. The assumption that the $\{F_i\}_{i=1}^M$ are arbitrary smooth mappings improves the flexibility of the triangulation, but does not make the analysis essentially different from the case of affine mappings. This is seen from the estimates in Section 3, where we have used only bounds on the Jacobian and inverse of the Jacobian of F_i. Therefore, without loss of generality, we assume, from now on, that the F_i are affine mappings. Throughout this subsection, u is a finite element function belonging to P^h.

For a proof of Lemma 4 and a general discussion, see Bramble and Xu [5].

LEMMA 4. *Let $Q^H u$ be the L^2 projection of $u \in P^h(\Omega)$ onto the coarse space V^H. Then,*

$$||u - Q^H u||^2_{L^2(\Omega)} \preceq H^2 |u|^2_{H^1(\Omega)},$$

and

$$|Q^H u|^2_{H^1(\Omega)} \preceq |u|^2_{H^1(\Omega)}.$$

We remark that these bounds are not necessarily independent of the values k_i of the coefficient. A sufficient condition to guarantee this independence is that the coefficients k_i satisfy a quasi-monotone condition; see [9].

In what follows, some of the results are stated for substructures of diameter proportional to H, but the arguments are given only for a reference substructure. The introduction of the scaling factors into the final formulas is, by the results of Section 3, routine.

LEMMA 5. *Let $\bar{u}_{\mathcal{W}_j}$ be the average value of u on $\mathcal{W}_j$, the wirebasket of subdomain Ω_j. Then*

$$||u||^2_{L^2(\mathcal{W}_j)} \preceq (1+\log(N))||u||^2_{H^1(\Omega_j)},$$

and

$$||u-\bar{u}_{\mathcal{W}_j}||^2_{L^2(\mathcal{W}_j)} \preceq (1+\log(N))|u|^2_{H^1(\Omega_j)}.$$

Similar bounds also hold for an individual substructure edge.

Proof. In the reference substructure, we know that $P^{\hat{h}} \subset V^{\hat{h}}$, where $P^{\hat{h}}$ was defined in Section 2, and $V^{\hat{h}}$ is a Q_1 finite element space defined on a shape-regular triangulation that is a refinement of $\mathcal{T}^{\hat{h}}$; we can refine all the elements of $\mathcal{T}^{\hat{h}}$ with sides bigger than, say, $3\hat{h}/2$, where $\hat{h} \asymp 1/N^2$. Now we apply Lemma 4.3 in [10], a well-known result for shape-regular triangulations, to get both estimates. □

In the abstract Schwarz convergence theory, the crucial point in the estimate of the rate of convergence of a two-level algorithm is the proof that all functions in the finite element space can be decomposed into components belonging to the subspaces, in such a way that the sum of the resulting energies are uniformly, or almost uniformly, bounded with respect to the parameters H and N. The main technique for deriving such a decomposition is the use of a suitable partition of unity. In the next two lemmas, we construct functions that are used to define such partitions of unity.

LEMMA 6. *Let $\mathcal{F}_k$ be the face common to Ω_i and Ω_j, and let $\theta_{\mathcal{F}_k}$ be the function in $P^h(\Omega)$ that is equal to one at the interior nodes of $\mathcal{F}_k$, zero at the remaining nodes of $\partial\Omega_i \cup \partial\Omega_j$, and discrete harmonic in Ω_i and Ω_j. Then*

$$|\theta_{\mathcal{F}_k}|^2_{H^1(\Omega_i)} \preceq (1+\log(N))H.$$

The same bound also holds for the other subregion Ω_j.

Proof. We define functions $\hat{\theta}_{\mathcal{F}_k}$ and $\hat{\vartheta}_{\mathcal{F}_k}$ in the reference cube; $\theta_{\mathcal{F}_k}$ and $\vartheta_{\mathcal{F}_k}$ are obtained, as usual, by mapping; see Section 3. We construct the function $\hat{\vartheta}_{\mathcal{F}_k}$ with the same boundary values as $\hat{\theta}_{\mathcal{F}_k}$, and then prove that the bound given in the Lemma holds for $\hat{\vartheta}_{\mathcal{F}_k}$. The standard energy minimizing property of discrete harmonic functions then gives the estimate for $\hat{\theta}_{\mathcal{F}_k}$. The six functions $\hat{\vartheta}_k$ which correspond to the six faces of the cube also form a partition of unity at all nodes belonging to the closure of the substructure except those on the wirebasket; this property is used in the next lemma.

We divide the substructure into twenty-four subtetrahedra by connecting its center C to all the vertices and to all the six centers C_k of the faces, and by drawing the diagonals of the faces of $\hat{\Omega}$; see Fig. 1.

The function $\hat{\vartheta}_{\mathcal{F}_k}$ associated with the face $\mathcal{F}_k$ is defined to be $1/6$ at the point C. The values at the centers of the faces are $\hat{\vartheta}_{\mathcal{F}_k}(C_j) = \delta_{jk}$, for $j = 1, ..., 6$, where δ_{jk} is the Kronecker symbol. $\hat{\vartheta}_{\mathcal{F}_k}$ is linear on the segments CC_j. The values inside each

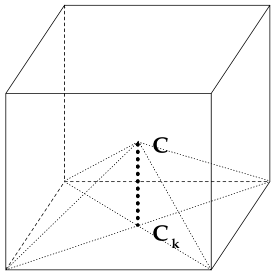

FIG. 1. *One of the segments CC_k*

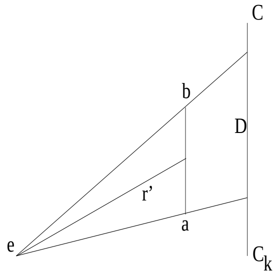

FIG. 2. *Geometry underlying equation (18)*

subtetrahedron formed by a segment CC_j and one edge of $\mathcal{F}_j$ are defined to be constant on the intersection of any plane through that edge, and are given by the value, already known, on the segment CC_j. Next, the whole function $\hat{\vartheta}_{\mathcal{F}_k}$ is modified to be a piecewise Q_1 function on $\mathcal{T}^{\hat{h}}$ by interpolating at the GLL nodes; the values of this finite element function at the nodes on the wirebasket are defined to be equal to zero.

We claim that $|\nabla \hat{\vartheta}_{\mathcal{F}_k}(x)| \leq C/r$, where x is a point belonging to any element $\hat{K}$ that does not touch any edge of the cube, and r is the distance from the center of $\hat{K}$ to the closest edge of the cube. Let $\overline{ab}$ be a side of $\hat{K}$. We analyze in detail the situation depicted in Fig. 2, where $\overline{ab}$ is parallel to CC_k. Let e be the intersection of the plane containing these two segments with the edge of the cube that is closest to $\overline{ab}$. Then $|\hat{\vartheta}_{\mathcal{F}_k}(b) - \hat{\vartheta}_{\mathcal{F}_k}(a)| \preceq D$, by the construction of $\hat{\vartheta}_{\mathcal{F}_k}$, where D is the size of the radial projection with center e of $\overline{ab}$ onto CC_k. By similarity of triangles, we may write:

$$|\hat{\vartheta}_{\mathcal{F}_k}(b) - \hat{\vartheta}_{\mathcal{F}_k}(a)| \preceq \frac{\mathrm{dist}(a,b)}{r'}, \tag{19}$$

where r' is the distance between e and the midpoint of $\overline{ab}$. Here we have used that the distance between e and CC_k is of order 1. If the segment $\overline{ab}$ is not parallel to CC_k, the difference $|\hat{\vartheta}_{\mathcal{F}_k}(b) - \hat{\vartheta}_{\mathcal{F}_k}(a)|$ is even smaller, and (19) is still valid. Notice that r' is within a multiple of 2 of r. Therefore Lemma 2 implies that $|\nabla \hat{\vartheta}_{\mathcal{F}_k}(x)| \leq C/r$.

In order to estimate the energy of $\hat{\vartheta}_{\mathcal{F}_k}$, we start with the elements $\hat{K}$ that touch an edge $\mathcal{E}$ of the cube. Let h_3 be the side of $\hat{K}$ which is parallel to $\mathcal{E}$. Then h_3 is greater than or equal to the other sides of $\hat{K}$, by the properties of the GLL nodes, as explained in Section 2. Since the nodal values of $\hat{\vartheta}_{\mathcal{F}_k}$ in $\hat{K}$ are bounded by 1, by the construction of $\hat{\vartheta}_{\mathcal{F}_k}$, we have:

$$|\hat{\vartheta}_{\mathcal{F}_k}|_{H^1(\hat{K})} \preceq h_3,$$

by using equation (16). Summing over $\hat{K}$, we conclude that the energy of $\hat{\vartheta}_{\mathcal{F}_k}$ is bounded independently of N for the union of all elements that touch the edges of the cube.

To estimate the contribution to the energy from the other elements of the substructure, we consider one subtetrahedron at a time and introduce cylindrical coordinates using the substructure edge, that belongs to the subtetrahedron, as the z-axis. The bound now follows from the bound on the gradient of $\hat{\vartheta}_{\mathcal{F}_k}$ given above and elementary considerations. We refer to [10] for more details, and also to the proof of the next lemma, where a similar computation is performed. □

The following lemma corresponds to Lemma 4.5 in [10]. This lemma and the previous one are the keys to avoiding the use of $H_{00}^{1/2}$ estimates and extension theorems in the analysis of our algorithms.

LEMMA 7. *Let $\vartheta_{\mathcal{F}_k}(x)$ be the function introduced in the proof of Lemma 6, let $\mathcal{F}_k$ be a face of the substructure Ω_j, and let I^h denote the interpolation operator associated with the finite element space P^h and the image of the GLL points under the mapping F_j. Then,*

$$\sum_k I^h(\vartheta_{\mathcal{F}_k} u)(x) = u(x),$$

for all nodal points $x \in \overline{\Omega}_j$ that do not belong to the wirebasket $\mathcal{W}_j$, and

$$|I^h(\vartheta_{\mathcal{F}_k} u)|^2_{H^1(\Omega_j)} \preceq (1+\log(N))^2 ||u||^2_{H^1(\Omega_j)}.$$

Proof. The first part is trivial from the construction of $\hat{\vartheta}_{\mathcal{F}_k}$ made in the previous lemma. For the second part, we work in the reference substructure, and first estimate the sum of the energy of all the elements $\hat{K}$ that touch an edge $\mathcal{E}$ of the wirebasket. We provide a detailed argument only for $\hat{K}$ touching $\mathcal{F}_k$; the other elements that touch an edge are treated similarly. The nodal values of $I^{\hat{h}}(\hat{\vartheta}_{\mathcal{F}_k}\hat{u})$ in such an element are 0,0,0,0, $\hat{u}(a)$, $\hat{u}(b)$, $\hat{\vartheta}_{\mathcal{F}_k}(c)\hat{u}(c)$ and $\hat{\vartheta}_{\mathcal{F}_k}(d)\hat{u}(d)$; $\hat{\vartheta}_{\mathcal{F}_k}$ lies between 0 and 1. Moreover, let h_3 be the side of $\hat{K}$ that is parallel to $\mathcal{E}$. Then $h_3 \succeq h_1$ and $h_3 \succeq h_2$, by the geometrical properties of the GLL mesh. Now, equation (16) implies:

$$|I^{\hat{h}}(\hat{\vartheta}_{\mathcal{F}_k}\hat{u})|^2_{H^1(\hat{K})} \preceq h_3(\hat{u}^2(a) + \hat{u}^2(b) + (\hat{\vartheta}_{\mathcal{F}_k}(c)\hat{u}(c))^2 + (\hat{\vartheta}_{\mathcal{F}_k}(d)\hat{u}(d))^2).$$

Then, applying (15) for the segments that are parallel to $\mathcal{E}$, and Lemma 5, we have:

$$\sum_{\hat{K}} |I^{\hat{h}}(\hat{\vartheta}_{\mathcal{F}_k}\hat{u})|^2_{H^1(\hat{K})} \preceq (1+\log(N))||\hat{u}||^2_{H^1(\Omega_j)},$$

where this sum is taken over all elements $\hat{K}$ that touch the wirebasket of $\hat{\Omega}$.

We next bound the energy of the interpolant for the other elements. By the proof of the previous lemma, $|\nabla\hat{\vartheta}_{\mathcal{F}_k}| \leq C/r$, where r is the distance between the element $\hat{K}$ and the nearest edge of $\hat{\Omega}$. Then, Lemma 3 implies that

$$\sum_{\hat{K}\subset\hat{\Omega}} |I^{\hat{h}}(\hat{\vartheta}_{\mathcal{F}_k}\hat{u})|^2_{H^1(\hat{K})} \preceq \sum_{\hat{K}\subset\hat{\Omega}} (|\hat{u}|_{H^1(\hat{K})} + r^{-2}||\hat{u}||^2_{L^2(\hat{K})}),$$

where the sum is taken over all elements $\hat{K}$ that do not touch the wirebasket of $\hat{\Omega}$.

The bound of the first term in the sum is trivial. To bound the second term, we partition the elements of $\hat{\Omega}$ into groups, in accordance to the closest edge of $\hat{\Omega}$; the exact rule for the assignment of the elements that are halfway between is of no importance. For each edge of the wirebasket, we use a local cylindrical coordinate system with the z axis coinciding with the edge, and the radial direction, r, normal to it. The sum restricted to each of these groups of elements can be estimated by an integral

$$\sum_{\hat{K}\subset\hat{\Omega}} r^{-2}||\hat{u}||^2_{L^2(\hat{K})} \preceq \int_{r=\hat{h}}^{C}\int_\theta\int_z (\hat{u})^2\frac{r}{r^2}\,dz\,d\theta\,dr.$$

The integral with respect to z can be bounded by using Lemma 5. We obtain

$$\sum_{\hat{K}\subset\hat{\Omega}} r^{-2}||\hat{u}||^2_{L^2(\hat{K})} \preceq (1+\log(C/\hat{h}))||\hat{u}||^2_{H^1(\hat{\Omega})}\int_{r=\hat{h}}^{C} r^{-1}dr$$

and thus

$$\sum_{\hat{K}\subset\hat{\Omega}} |I^{\hat{h}}(\hat{\vartheta}_{\mathcal{F}_k}\hat{u})|^2_{H^1(\hat{K})} \preceq (1+\log(C/\hat{h}))^2||\hat{u}||^2_{H^1(\hat{\Omega})}.$$

□

We note that this proof is an extension of an argument given in [10] for shape-regular meshes, and that equation (17) replaces the use of the inverse inequality, which if used here would introduce the bad aspect ratios of the elements into the estimates.

LEMMA 8. *Let $\bar{u}_{\partial\mathcal{F}_k}$, and $\bar{u}_{\mathcal{W}_j}$ be the averages of u on $\partial\mathcal{F}_k$, and $\mathcal{W}_j$, respectively. Then,*

$$(\bar{u}_{\partial\mathcal{F}_k})^2 \preceq \frac{1}{H}||u||^2_{L^2(\partial\mathcal{F}_k)},$$

$$(\bar{u}_{\mathcal{W}_j})^2 \preceq \frac{1}{H}||u||^2_{L^2(\mathcal{W}_j)}.$$

The proof is a direct consequence of the Cauchy–Schwarz inequality.

LEMMA 9. *Let $u \in P^h(\Omega_i)$ be zero on the mesh points of the faces of Ω_j and discrete harmonic in Ω_j. Then,*

$$|u|^2_{H^1(\Omega_j)} \preceq ||u||^2_{L^2(\mathcal{W}_j)}.$$

This result follows by estimating the energy norm of the zero extension of the boundary values using equation (16) and by noting that the harmonic extension has a smaller energy.

5. Iterative Substructuring Algorithms. At this point, we can propose and analyze several iterative substructuring methods previously developed for finite elements. We choose the wirebasket algorithm proposed by Smith [31] because it is efficient, and its analysis raises all the important technical issues. In a practical problem, the choice between the many alternatives now known should be made on the basis of the theoretical results that can be derived from our theory, as well as numerical experimentation.

Smith's algorithm is a wirebasket based method, and it is also described as Algorithm 6.4 in [10] in the context of standard finite elements. It can be viewed as a block-diagonal preconditioner after transforming S_h into a convenient basis, and the same is true for our algorithm.

By the abstract framework of Schwarz methods developed for example in [10], we know that in order to describe the algorithm we only need to prescribe subspaces, the sum of which spans the whole space of h-discrete harmonic functions of $P_0^h(\Omega)$, and one bilinear form for each subspace.

For each internal face $\mathcal{F}_k$, we let $V_{\mathcal{F}_k}$ be the space of h-discrete harmonic functions that vanish at all the interface nodes that do not belong to this face. The functions in $V_{\mathcal{F}_k}$ have support in $\overline{\Omega}_{ij}$, the union of the two substructures $\overline{\Omega}_i$ and $\overline{\Omega}_j$ that share the face $\mathcal{F}_k$. The bilinear form used for these spaces is $a(\cdot,\cdot)$.

The wirebasket subspace is the range of the following interpolation operator:

$$I_W^h u = \sum_{x_k \in \mathcal{W}_h} u(x_k)\varphi_k + \sum_k \bar{u}_{\partial F^k}\theta_{F^k}.$$

Here, φ_k is the discrete harmonic extension of the standard nodal basis functions ϕ_k, $\mathcal{W}_h$ is the set of nodes in the union of all the wirebaskets, and $\bar{u}_{\partial F^k}$ is the average of u on ∂F^k. The bilinear form for this coarse subspace is given by

$$b_0(u,u) = (1+\log(N))\sum_i k_i \inf_{c_i} ||u-c_i||^2_{L^2(\mathcal{W}_i)}.$$

These subspaces and bilinear forms define, via the Schwarz framework, a preconditioner of S_h that we call $\tilde{S}_{h,WB}$.

THEOREM 1. *For the preconditioner $\tilde{S}_{h,WB}$, we have*

$$\kappa(\tilde{S}_{h,WB}^{-1}S_N) \preceq (1+log(N))^2,$$

where the constant C is independent of N, H, and the values k_i of the coefficient.

Proof. We can apply, word by word, the proof of theorem 6.4 in [10] to the matrix S_h, using now the tools developed in Section 4. This gives

$$\kappa(\tilde{S}_{h,WB}^{-1}S_h) \preceq (1+log(N))^2.$$

The harmonic FEM-SEM equivalence (13) and a Rayleigh quotient argument complete the proof; see Section 3. □

The next algorithm is obtained from the previous one by the discrete harmonic FEM-SEM equivalence, by which we find a preconditioner $\tilde{S}_{N,WB}$ from $\tilde{S}_{h,WB}$. The subspaces that define the preconditioner are now contained in the space of Q-discrete harmonic functions of $P_0^N(\Omega)$.

Each face subspace, related to a face $\mathcal{F}_k$, consists of the set of all Q-discrete harmonic functions that are zero at all the interface nodes that do not belong to the interior of the face $\mathcal{F}_k$. The bilinear form for these spaces is $a_Q(\cdot,\cdot)$.

The wirebasket subspaces are defined as before, by prescribing the values at the GLL(N) nodes on a face as the average of the function on the boundary of the face. The bilinear form used for the wirebasket subspace is $b_0^Q(\cdot,\cdot)$, obtained from $b_0(\cdot,\cdot)$ by applying the GLL(N) quadrature to compute the L^2-norm on each edge of the wirebasket. This is exactly the wirebasket method based on GLL quadrature described in [27].

The following lemma shows the equivalence of the two functions u_h and u_N with respect to the bilinear forms $b_0(\cdot,\cdot)$ and $b_0^Q(\cdot,\cdot)$, respectively.

LEMMA 10. *Let u_h be a Q_1 finite element function on the GLL(N) mesh on the interval $I = [-1, +1]$, and let u_N be its polynomial interpolant using the nodes of this mesh. Then,*

$$\inf_c ||u_h - c||^2_{L^2(I)} \asymp \inf_c \sum_{j=0}^{N} (u_N(\xi_j) - c)^2 \rho_j$$

Proof. The GLL(N) quadrature has the following important property:
For any polynomial u_N of degree N defined on I,

$$||u_N||^2_{L^2(\Lambda)} \leq \sum_{j=0}^{N} u_N^2(\xi_j)\rho_j \leq 3||u_N||^2_{L^2(\Lambda)};$$

see [1, p. 75]. Therefore, it is enough to prove that:

$$\inf_c ||u_h - c||^2_{L^2(I)} \asymp \inf_c ||u_N - c||^2_{L^2(I)}.$$

We prove only the $\preceq$ part of this last estimate, since the opposite inequality is analogous. The inequality without the infimum is valid for the constant c_r that realizes the inf in the right hand side by the FEM-SEM equivalence. By taking the inf of the left hand side the inequality is preserved. □

THEOREM 2. *For the preconditioner $\tilde{S}_{N,WB}$, we have*

$$\kappa(\tilde{S}^{-1}_{N,WB} S_N) \preceq (1 + \log(N))^2$$

where the constant is independent of the parameters H, N, and the values k_i of the coefficient.

Proof. In this proof, the functions with indices h and N are h- and Q- discrete harmonic functions respectively, and they agree at the GLL nodes that belong to the interface Γ. As observed in Section 3, it is enough to analyze one substructure Ω_i at a time, and prove the following equivalence:

$$b^Q_{0,\mathcal{W}_i}(u_N, u_N) + \sum_{\mathcal{F}_k \subset \Omega_i} k_i |u_N - \overline{u}_{N,\partial\mathcal{F}_k} \theta_{N,\mathcal{F}_k}|^2_{H^1(\Omega_i)} \asymp b_{0,\mathcal{W}_i}(u_h, u_h) + \sum_{\mathcal{F}_k \subset \Omega_i} k_i |u_h - \overline{u}_{h,\partial\mathcal{F}_k} \theta_{h,\mathcal{F}_k}|^2_{H^1(\Omega_i)}, \tag{20}$$

where the subscript $\mathcal{W}_i$ means that only the contribution from the wirebasket of Ω_i is used to define the bilinear form. We prove only the $\preceq$ part; the proof of the reverse inequality is analogous. We first note that Lemma 10 bounds the first term on the left hand side by the first term on the right hand side.

Each term in the sum on the left hand side can be bounded from above by

$$2k_i |u_N - \overline{u}_{h,\partial\mathcal{F}_k} \theta_{N,\mathcal{F}_k}|^2_{H^1(\Omega_i)} + 2k_i |(\overline{u}_{h,\partial\mathcal{F}_k} - \overline{u}_{N,\partial\mathcal{F}_k}) \theta_{N,\mathcal{F}_k}|^2_{H^1(\Omega_i)}.$$

The first term of this expression can be bounded from above by the corresponding term on the right hand side by using the harmonic FEM-SEM equivalence. The second term is bounded by

$$Ck_i H(1 + \log(N)) |\overline{u}_{h,\partial\mathcal{F}_k} - \overline{u}_{N,\partial\mathcal{F}_k}|^2 = Ck_i H(1 + \log(N)) |\overline{(u_h - c_{h,\mathcal{W}_i})}_{\partial\mathcal{F}_k} - \overline{(u_N - c_{h,\mathcal{W}_i})}_{\partial\mathcal{F}_k}|^2,$$

where $c_{h,\mathcal{W}_i}$ is the average of u_h over $\mathcal{W}_i$. Here we have used that the estimate on the energy norm of $\theta_{h,\mathcal{F}_k}$, given in Lemma 6, implies a similar estimate for $\theta_{N,\mathcal{F}_k}$, by (13). Applying the Cauchy-Schwarz inequality, as in Lemma 8, and the FEM-SEM equivalence, we can bound this last expression in terms of the first term of the right hand side of equation (20). □

6. Overlapping Schwarz Algorithms. We now consider the additive overlapping Schwarz method, which is presented, e.g., in [11, 12]. We recall that an abstract framework, given in Theorem 3.1 of [11], is available for the analysis of this type of algorithm. Here we only discuss the additive version, but the analysis can also be extended in a standard way to the multiplicative variant [4], which has proven more effective in many practical problems.

As in the previous section, a preconditioner $\tilde{K}_h$ for K_h is specified by a set of local spaces together with a coarse space. We also have to provide bilinear forms (approximate solvers) for the elliptic problems restricted to each of these subspaces. Here we work with exact solvers, i.e. the bilinear form is $a(\cdot,\cdot)$. The extension to approximate solvers is straightforward.

In the context of spectral elements, the following construction was first proposed by Pahl [22]. The domain Ω is covered by substructures Ω_i, which are the original spectral elements. We enlarge each of them, to produce overlapping subregions Ω_i', in such a way that the boundary of Ω_i' does not cut through any element of the triangulation $\mathcal{T}^h$ generated by the GLL nodes. The overlap δ is the minimum distance between the boundaries of Ω_i and Ω_i'. When δ is proportional to H the overlap is called generous, and when δ is comparable to the size of the elements of $\mathcal{T}^h$, we speak of a small overlap. For the sake of simplicity, we again restrict our analysis to the case when all the mappings F_i are affine. The general situation can be treated similarly.

The local spaces are given by $P_0^h(\Omega_i')$, the set of functions in $P_0^h(\Omega)$ that vanish at all the nodes on or outside $\partial\Omega_i'$. The coarse space is the Q_1 finite element space defined on the mesh generated by the subregions Ω_i, the elements of the coarse triangulation, which are shape-regular by assumption; see Section 2. This setting incorporates both small and generous overlap.

THEOREM 3. *Pahl's additive Schwarz algorithm satisfies:*

$$\kappa(\tilde{K}_{h,AS}^{-1}K_N) \preceq (1 + H/\delta)$$

The constant C is independent of the parameters H, N, and δ.

Proof. As before, we follow the proof of the analogous theorem for shape-regular finite elements; see Theorem 3 in [12]. The proof applies, word by word, except for the estimate of $a_K(I_h(\theta_i w_h), I_h(\theta_i w_h))$ where I_h is the interpolation operator, $\{\theta_i\}$ a partition of unity (different from the one described in Lemma 6), w_h a finite element function, and $a_K(\cdot,\cdot)$ the restriction of $a(\cdot,\cdot)$ to the single element $K \in \mathcal{T}^h$. It is known that θ_i can be found such that $|\theta_i| \le C$, and $|\nabla\theta_i| \le C/\delta$. Lemma 3 gives:

$$a_K(I_h(\theta_i w_h), I_h(\theta_i w_h)) \le C(|w_h|^2_{H^1(K)} + \frac{1}{\delta^2}\|w_h\|^2_{L^2(K)}),$$

where the constant C depends on the coefficients k_i. The rest of the proof follows without any change, and we obtain

$$\kappa(\tilde{K}_{h,AS}^{-1}K_h) \le C(1 + H/\delta).$$

The FEM-SEM equivalence and a Rayleigh quotient argument complete the proof. □

REMARK 1. *Even though the theory does not rule out the possibility of growth of the constant C of Theorem 3 when the coefficient $k(x)$ has large jumps, only a very moderate increase has been observed in numerical experiments; see e.g. [15]. We also note that when the overlap is generous, the method is optimal in the sense that the condition number is uniformly bounded with respect to N and H.*

REMARK 2. *In the present algorithm, the local spaces are allowed to be more general than those considered by Pavarino [24, 25, 26]. For each crosspoint x_ℓ, Pavarino defines an extended subdomain Ω'_ℓ as the union of all the subdomains that contain x_ℓ as a vertex. Therefore, δ is always on the order of H.*

We now apply the FEM-SEM equivalence to the subspaces that define $\tilde{K}_{h,AS}$, to propose yet another preconditioner; this is the same technique used to derive the preconditioner $\tilde{S}_{N,WB}$ from $\tilde{S}_{h,WB}$. The coarse space is the same as the one for $\tilde{K}_{h,AS}$, while the local spaces are given by

$$V^N_{\Omega'_i} = \{v_N \in P^N_0(\Omega) \text{ such that } I^h_N(v_N) \in P^h_0(\Omega'_i)\}.$$

Notice that the polynomials of $V^N_{\Omega'_i}$ are generally not equal to zero outside Ω'_i, and therefore $V^N_{\Omega'_i} \not\subset P^N_0(\Omega'_i)$.

These subspaces and the use of the bilinear forms $a_Q(\cdot,\cdot)$ and $a(\cdot,\cdot)$ for the local and coarse spaces, respectively, define our new preconditioner $\tilde{K}_{N,AS}$. Theorem 3 and a simple application of the FEM-SEM equivalence for each of the local spaces immediately give:

THEOREM 4.

$$\kappa(\tilde{K}^{-1}_{N,AS} K_N) \leq C(1 + H/\delta).$$

REMARK 3. *To the best of our knowledge, this preconditioner $\tilde{K}_{N,AS}$ is new. Even though $\tilde{K}_{h,AS}$ is superior to $\tilde{K}_{N,AS}$ for the model problem considered here, because the local problems are much easier to solve, the comparative efficiency in more complicated problems can only be determined by experiments.*

7. Comments on the Numerical Experiments by Pahl. We describe here some of the experiments performed by Pahl [22]. These experiments have motivated our analysis, and are used to illustrate the efficiency of some of the algorithms considered in the last two sections. For more details on this very thorough study, we refer to [22].

The region Ω was taken to be the unit square in the plane, and the tests were based on the two dimensional analogues of the methods described in the previous two sections. Ω was subdivided into a uniform $M \times M$ mesh of squares, with sides $H = 1/M$. In each square, polynomials of degree N were used. The coefficient $k(x)$ was equal to one, and the right hand side of (1) was chosen so that the exact solution was $u = xy(1-x)(1-y)$. The stopping criterion for the PCG iteration was a reduction of 10^{-5} in the Euclidean norm of the residual, and only iteration counts were reported. The experiments were performed for the finite element based preconditioners of the spectral element stiffness matrix; see our Theorems 1 and 3.

In a first set of experiments, the iterative substructuring methods were considered. Several preconditioners were studied. We focus our attention on the wirebasket preconditioner analyzed in Section 5, and an analogue of the balancing preconditioner of

Mandel and Brezina [20]. For $N = 4$ and M between 2 and 12, the number of iterations was bounded by 10, and grew hardly at all, with increasing M. For $M = 7$ and N between 4 and 12, the iteration count increased very slowly with N, and was bounded by 11 for the wirebasket and balancing preconditioners. We remark that the analysis of the finite element balancing preconditioner for the spectral element method is a straightforward application of the results of Section 5 and the existing theory for shape-regular finite elements. Pahl's results corroborate, in a clear cut way, the results of the theory.

The overlapping Schwarz preconditioner was studied in a second set of experiments. The domain was divided as before into $M \times M$ subdomains, polynomials of degree N were used within each subdomain, and δ was taken to be on the order of one or two mesh intervals. From the geometrical properties of the GLL mesh, it is easy to see that the bound on the condition number given by Theorem 3 grows like $(1 + H/\delta) \asymp N^2$. Hence, our theory predicts an iteration count which is linear in N and independent of M. The experiments performed by Pahl showed that for $N = 4$, the number of iterations grows very slowly with M between 2 and 12, and presents a sublinear growth when N increases from 4 to 12, for $M = 7$. The maximum iteration count was 22, achieved for $M = 7$ and $N = 12$. Our estimate seems pessimistic in its dependence on N, at least for this range of values, while it describes the dependence on the number of subdomains quite well.

An important practical question, also addressed by Pahl's experiments, is the choice of the most efficient overlap δ for a particular problem and decomposition of the domain. The greater the overlap, the smaller the iteration count, but since a more generous overlap also increases the work to solve the local problems, it is hard to decide in advance what the best δ would be. The results obtained by Pahl indicate that, for $M = 7$ and N between 4 and 9, one mesh size overlap appears to be a good choice in terms of total work on a serial machine, while a more generous overlap seems to be appropriate for larger N.

Acknowledgements. I wish to thank my advisor Olof Widlund, for all his encouragement, and my colleagues Shannon Pahl, Axel Klawonn, Luca Pavarino, and Marcus Sarkis, for many conversations about this project.

REFERENCES

[1] C. Bernardi and Y. Maday, *Approximations Spectrales de Problèmes aux Limites Elliptiques*, vol. 10 of Mathèmatiques & Applications, Springer-Verlag France, Paris, 1992.

[2] C. Bernardi and Y. Maday, *Polynomial interpolation results in Sobolev spaces*, J. Comput. Appl. Math., 43 (1992), pp. 53 – 80.

[3] J. H. Bramble, J. E. Pasciak, and A. H. Schatz, *The construction of preconditioners for elliptic problems by substructuring, IV*, Math. Comp., 53 (1989), pp. 1–24.

[4] J. H. Bramble, J. E. Pasciak, J. Wang, and J. Xu, *Convergence estimates for product iterative methods with applications to domain decomposition*, Math. Comp., 57 (1991), pp. 1–21.

[5] J. H. Bramble and J. Xu, *Some estimates for a weighted L^2 projection*, Math. Comp., 56 (1991), pp. 463–476.

[6] C. Canuto, *Stablization of spectral methods by finite element bubble functions*, Comput. Methods Appl. Mech. Engrg, 116 (1994), pp. 13–26. Proceedings of ICOSAHOM 92, a conference held in Montpellier, France, June 1992.

[7] C. Canuto and D. Funaro, *The Schwarz algorithm for spectral methods*, SIAM J. Numer. Anal., 25 (1988), pp. 24–40.

[8] M. O. Deville and E. H. Mund, *Finite-element preconditioning for pseudospectral solutions of elliptic problems*, Siam J. Sci. Stat. Comput., 11 (1990), pp. 311 – 342.

[9] M. Dryja, M. Sarkis, and O. B. Widlund, *Multilevel Schwarz methods for elliptic problems with discontinuous coefficients in three dimensions*, Tech. Rep. 662, Department of Computer Science, Courant Institute, March 1994. To appear in Numer. Math.

[10] M. Dryja, B. F. Smith, and O. B. Widlund, *Schwarz analysis of iterative substructuring algorithms for elliptic problems in three dimensions*, SIAM J. Numer. Anal., 31 (1994), pp. 1662–1694.

[11] M. Dryja and O. B. Widlund, *Additive Schwarz methods for elliptic finite element problems in three dimensions*, in Fifth International Symposium on Domain Decomposition Methods for Partial Differential Equations, D. E. Keyes, T. F. Chan, G. A. Meurant, J. S. Scroggs, and R. G. Voigt, eds., Philadelphia, PA, 1992, SIAM, pp. 3–18.

[12] ———, *Domain decomposition algorithms with small overlap*, SIAM J. Sci.Comput., 15 (1994), pp. 604–620.

[13] S. C. Eisenstat, M. H. Schultz, and A. H. Sherman, *Applications of an element model for Gaussian elimination*, in Sparse Matrix Computations, J. R. Bunch and D. J. Rose, eds., Academic Press, 1976, pp. 85–96.

[14] P. F. Fischer and E. Rønquist, *Spectral element methods for large scale parallel Navier-Stokes calculations*, Comput. Methods Appl. Mech. Engrg, 116 (1994), pp. 69–76. Proceedings of ICOSAHOM 92, a conference held in Montpellier, France, June 22-26, 1992.

[15] W. D. Gropp and B. F. Smith, *Experiences with domain decomposition in three dimensions: Overlapping Schwarz methods*, in Domain Decomposition Methods in Science and Engineering: The Sixth International Conference on Domain Decomposition, A. Quarteroni, Y. A. Kuznetsov, J. Périaux, and O. B. Widlund, eds., vol. 157, AMS, 1994, pp. 323–334. Held in Como, Italy, June 15–19,1992.

[16] D. E. Keyes, T. F. Chan, G. A. Meurant, J. S. Scroggs, and R. G. Voigt, eds., *Fifth International Symposium on Domain Decomposition Methods for Partial Differential Equations*, Philadelphia, PA, 1992, SIAM. Held in Norfolk, VA, May 6–8, 1991.

[17] D. E. Keyes and J. Xu, eds., *Domain Decomposition Methods in Science and Engineering*, vol. 180, Providence, R.I., 1994, AMS. Proceedings of the Seventh International Conference on Domain Decomposition, October 27-30, 1993, The Pennsylvania State University.

[18] Y. Maday, D. Meiron, A. T. Patera, and E. M. Rønquist, *Analysis of iterative methods for the steady and unsteady Stokes problem: Application to spectral element discretizations*, SIAM J. Sci. Comp., 14 (1993), pp. 310–337.

[19] Y. Maday and A. T. Patera, *Spectral element methods for the Navier-Stokes equations*, in State of the Art Surveys in Computational Mechanics, A. Noor and J. Oden, eds., New York, 1989, ASME.

[20] J. Mandel and M. Brezina, *Balancing domain decomposition: Theory and computations in two and three dimensions*, Tech. Rep. UCD/CCM 2, Center for Computational Mathematics, University of Colorado at Denver, 1993.

[21] S. A. Orzag, *Spectral methods for problems in complex geometries*, Journal of Computational Physics, 37 (1980), pp. 70–92.

[22] S. S. Pahl, *Schwarz type domain decomposition methods for spectral element discretizations*, Master's thesis, Department of Computational and Applied Mathematics, University of the Witwatersrand, Johannesburg, South Africa, December 1993.

[23] S. V. Parter and E. E. Rothman, *Preconditioning Legendre spectral collocation approximation to elliptic problems*, SIAM J. Numer. Anal., 32 (1995).

[24] L. F. Pavarino, *Domain Decomposition Algorithms for the p-version Finite Element Method for Elliptic Problems*, PhD thesis, Courant Institute, New York University, September 1992.

[25] ———, *Additive Schwarz methods for the p-version finite element method*, Numer. Math., 66 (1994), pp. 493–515.

[26] ———, *Schwarz methods with local refinement for the p-version finite element method*, Numer. Math., 69 (1994), pp. 185–211.

[27] L. F. Pavarino and O. B. Widlund, *Iterative substructuring methods for spectral elements: Problems in three dimensions based on numerical quadrature*, Tech. Rep. 663, Courant Institute of Mathematical Sciences, Department of Computer Science, May 1994. To appear in Computers Math. Applic.

[28] ———, *A polylogarithmic bound for an iterative substructuring method for spectral elements in three dimensions*, Tech. Rep. 661, Courant Institute of Mathematical Sciences, Department

of Computer Science, March 1994. To appear in SIAM J. Numer. Anal.

[29] A. Quarteroni, Y. A. Kuznetsov, J. Périaux, and O. B. Widlund, eds., *Domain Decomposition Methods in Science and Engineering: The Sixth International Conference on Domain Decomposition*, vol. 157, AMS, 1994. Held in Como, Italy, June 15–19,1992.

[30] A. Quarteroni and E. Zampieri, *Finite element preconditioning for legendre spectral collocation approximations to elliptic equations and systems*, SIAM J. Numer. Anal., 29 (1992), pp. 917 – 936.

[31] B. F. Smith, *A domain decomposition algorithm for elliptic problems in three dimensions*, Numer. Math., 60 (1991), pp. 219–234.